Multi-Antenna Covert Communication via Full-Duplex Jamming Against a Warden With Uncertain Locations

Xinying Chen, *Graduate Student Member, IEEE,* Wen Sun, *Senior Member, IEEE,* Chengwen Xing, *Member, IEEE,* Nan Zhao, *Senior Member, IEEE,* Yunfei Chen, *Senior Member, IEEE,* F. Richard Yu, *Fellow, IEEE,* and Arumugam Nallanathan, *Fellow, IEEE*

***Abstract*—Covert communication can hide the information transmission process from the warden to prevent adversarial eavesdropping. However, it becomes challenging when the location of warden is uncertain. In this paper, we propose a covert communication scheme against a warden with uncertain locations, which maximizes the connectivity throughput between a multi-antenna transmitter and a full-duplex jamming receiver with the limit of covert outage probability (the probability of the transmission found by the warden). First, we analyze the monotonicity of the covert outage probability to obtain the optimal location for the warden. Then, under this worst situation, we optimize the transmission rate, the transmit power and the jamming power of covert communication to maximize the connection throughput. This problem is solved in two stages. First, we derive the transmit-to-jamming power ratio limit from the maximum allowed covert outage probability. With this constraint, the connection probability is maximized over the transmit-to-jamming power ratio for a fixed transmission rate. Since the connection probability and the transmission rate are coupled, the bisection method is applied to maximize the connectivity throughput via optimizing the transmission rate iteratively. Simulation results are presented to evaluate the effectiveness of the proposed scheme.**

***Index Terms*—Active warden, artificial jamming, covert communication, full-duplex, low probability of detection.**

I. Introduction

The booming of Internet-of-Things (IoT) brings convenience to people's lives but also raises the concern on data privacy [1]. With the extremely large amount of personal data in the open wireless networks, wireless transmission is at the risk of adversarial eavesdropping. In order to protect wireless privacy, many researchers have worked on the physical layer security (PLS), e.g., beamforming [2]–[4], artificial jamming [5]–[8], and polarization [9], [10], *etc*. However, PLS alone is not enough, as it only prevents the eavesdropping but does not hide the existence of communication. In this regard, covert communication is emerging [11]. The work in [12] gave the theoretical information transmission limits, which made covert communication popular. Following these results, more works on covert communication have been conducted [13], [14]. Also, many works focused on the performance improvement of covert communication in different scenarios. For example, He *et al.* investigated the covert communication under both the finite and the infinite noise uncertainty in [15]. Hu *et al.* studied the covert communication of a greedy relay for its own message when forwarding the information from the source to the destination in [16]. In [17], Zhou *et al.* utilized the location uncertainty to exploit covert communication in unmanned aerial vehicle assisted networks and jointly optimized the trajectory and transmit power to achieve maximum average covert rate. Yan *et al.* presented the important features related to covert communication and discussed the practical challenges of future research in [18].

The advantages of multiple antennas have also been exploitedat different users to improve the their own performance in covert communication [19]–[23]. In [19], Shahzad *et al.* found that increasing the antennas equipped at the adversary Willie can reduce the covert throughput with the delay constraint. Zheng *et al.* investigated the covert communication with a multi-antenna transmitter and randomly distributed interferers and wardens under the centralized and distributed antenna systems in [20]. In [21], a multi-antenna beam sweeping based detection scheme was proposed by Hu *et al.*, where the Pinsker's inequality and Kullback-Leibler divergence were adopted to derive the detection error probability. Multiple antennas were applied for both the receiver and the jammer by Shmuel *et al.* in [22] to guarantee the covert communication. In [23], Shmuel *et al.* proposed that a multi-antenna jammer can maximize its assistance to the covert communication via performing beamforming towards a single direction with all available power.

On the other hand, artificial noise (AN) can also be adopted

Manuscript received October 8, 2020; revised January 28, 2021; accepted March 18, 2021. The work was supported by the National Key R&D Program of China under Grant 2020YFB1807002, and the National Natural Science Foundation of China (NSFC) under Grant 61871065. The associate editor coordinating the review of this paper and approving it for publication was H. Pishro-Nik. *(Corresponding author: Nan Zhao.)*

X. Chen and N. Zhao are with the Key Laboratory of Intelligent Control and Optimization for Industrial Equipment of Ministry of Education, Dalian University of Technology, Dalian 116024, China, and also with Peng Cheng Laboratory, Shenzhen 518066, China. (email: cxy@mail.dlut.edu.cn, zhaonan@dlut.edu.cn)

W. Sun is with the School of Cybersecurity, Northwestern Polytechnical University, Xi'an, 710129, China. (email: sunwen@nwpu.edu.cn)

C. Xing is with the School of Information and Electronics, Beijing Institute of Technology, Beijing 100081, China (e-mail:xingchengwen@gmail.com)

Y. Chen is with the School of Engineering, University of Warwick, Coventry CV4 7AL, U.K. (email: Yunfei.Chen@warwick.ac.uk)

F. R. Yu is with the Department of Systems and Computer Engineering, Carleton University, Ottawa, ON, K1S 5B6, Canada. (email: richard.yu@carleton.ca)

A. Nallanathan is with the School of Electronic Engineering and Computer Science, Queen Mary University of London, London E1 4NS, U.K. (email: a.nallanathan@qmul.ac.uk)

to confuse the warden by introducing more uncertainty on time and location [24], [25]. In [24], Soltani *et al.* derived the maximum bits that can be covertly transmitted according to the square root law when the friendly jammer is distributed as a two-dimensional Poisson point to disturb the warden. In [25], Liu *et al.* presented new results related to the active warden in the "shadow network" formed by the noisy wireless interference. In addition, the jamming power can be randomly changed to further improve the covert performance [26]–[28]. Some fundamental work was conducted in [26] to generate AN at the legitimate node that is closest to the warden, and thus a significant improvement can be achieved for covert communication. Shahzad *et al.* proposed a strategy to aid the covert communication in [27], where the receiver generates AN with varying power as a full-duplex receiver to cause uncertainty at the warden. Hu *et al.* applied the channel inversion power control in [28] to vary the power and phase based on the channel to the full-duplex jamming receiver to improve the performance in a covert wireless network.

Although the performance of covert communication can be enhanced either by multiple antennas or full-duplex jamming, there has been no existing work combining them. In addition, when the warden can determine an optimal location for detection, it also imposes a great challenge to the covert communication. The uncertainty of location information has been investigated in PLS [29] and in covert communications [17], [30], but none of the existing works consider a warden who can choose his optimal location in multi-antenna covert communications. Thus, in this paper, we focus on the use of multiple antennas with full-duplex jammer against a warden with uncertain locations. The key motivation and contribution of this paper are summarized as follows.

- To the best of our knowledge, the uncertain locations of a warden who can choose his optimal location in covert communication has not been studied. This remains a great challenge due to the high covert outage probability. In this paper, we will derive the optimal location and detection threshold for the warden, which brings more threat to the transmitter being detected. In addition, the warden can also change his locations to avoid being found.
- Under this worst situation, we propose a two-stage scheme to balance the tradeoff and maximize the connection probability with a fixed transmission rate while limiting the covert outage probability. Then, the maximization of the connection throughput is transformed into an optimization problem with only the transmission rate to be decided.
- The monotonicity of connection throughput over the transmission rate is analyzed. We will use the bisection method to obtain the optimal transmission rate between the transmitter and the receiver to maximize their connection throughput while guaranteeing the covertness.

The rest of the paper is organized as follows. In Section II, we present the system model. The detection and hypothesis testing are narrated in Section III, followed by the optimal location and power threshold for the warden in Section IV. In Section V, the optimal transmission rate is derived to maximize the connection throughput in covert communication. Simulation results are presented in Section VI, followed by conclusions in Section VII.

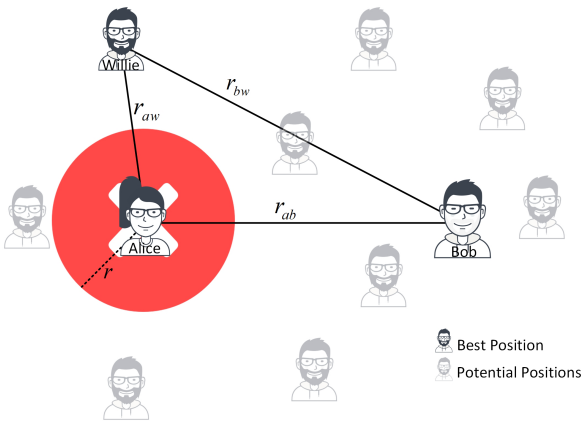

Fig. 1. Illustration of the covert communication between a multi-antenna Alice and a full-duplex jamming Bob under the surveillance of a Willie with uncertain locations.

Notation: Boldface lowercase and uppercase letters represent vectors and matrices. $\mathbb{C}^{M\times N}$ and $\mathcal{X} \triangleq [x, y]^T \in \mathbb{R}^{2\times 1}$ identify the $M \times N$ complex matrix and the location coordinate. $\mathbf{a}^T$, $\mathbf{a}^\dagger$ and $\|\mathbf{a}\|$ are the transpose, conjugate transpose and Euclidean norm of vector $\mathbf{a}$, respectively. $|c|$ and $\ln(*)$ are the absolute norm of the complex c and the natural logarithm. $\mathbb{P}\{*\}$, $\mathbb{E}_x[*]$, $f_x\{*\}$ and $\mathcal{F}_x\{*\}$ denote the probability, the expectation, the probability density function (PDF) and the cumulative distribution function (CDF) the random variable x.

II. System Model

Consider a wireless network with three nodes, Alice, Bob, and a Willie with uncertain locations, as shown in Fig. 1. Alice works as a transmitter equipped with M antennas. The full-duplex Bob receives the private information from Alice through one antenna and transmits AN via another antenna[1]. Bob himself is the AN source. Thus, he can rebuild and then eliminate the AN. However, due to the computational complexity limitation and practical constraint, perfect self-interference cancellation cannot be achieved, i.e., Bob still has $P_b\phi$ artificial noise left. P_b is the jamming power and ϕ is the self-interference cancelation ratio, $0 < \phi \leq 1$, which represents the proportion of the remaining AN power from Bob after its rebuilding and elimination. On the other hand, the single-antenna Willie wanders around trying to detect the covert communication between Alice and Bob. Specifically, equipping with a single antenna can improve the mobility of Willie and make itself difficult to be discovered by Alice. Without loss of generality, we apply two-dimensional Cartesian coordinates to denote the locations of Alice, Bob and Willie as $\mathcal{A} \triangleq [x_a, y_a]^T$, $\mathcal{B} \triangleq [x_b, y_b]^T$ and $\mathcal{W} \triangleq [x_w, y_w]^T$, respectively. Assume that Willie has the location knowledge of Alice. Willie can change his detection locations to perform

[1]The necessary information for Bob to perform the full-duplex jamming and receiving can be obtained in the header of each frame.

a better detection or avoid being discovered. To avoid being found by Alice, he has to keep a distance of at least r from Alice, which can be set according to the experience and environmental parameters, and will be specified in Section VI. Besides, to enable signal detection, he has to stay within the detection radius r_0 of Alice, which can be derived according to its minimum detectable signal power.

A. Channel Model

Assume that all the channel coefficients, except for the self-interfering coefficient h_{bb} of Bob, follow a large-scale path-loss with quasi-static Rayleigh fading. The complex channel coefficients from the i-th antenna of Alice to Willie and Bob can be denoted as $\sqrt{\frac{\rho_0}{r_{aw}^{\alpha}}}h_{a_iw}$ and $\sqrt{\frac{\rho_0}{r_{ab}^{\alpha}}}h_{a_ib}$, respectively, where h_{a_iw} and h_{a_ib} are the fading coefficients, r_{aw} and r_{ab} denote the distances from Alice to Willie and from Alice to Bob, respectively. ρ_0 denotes the reference power gain at a distance of 1 m, and α represents the path-loss exponent. The self-interfering channel coefficient h_{bb} of Bob follows quasi-static Rayleigh fading. h_{a_iw}, h_{a_ib}, h_{bw}, and h_{bb} are all independent and identically distributed (i.i.d.) complex Gaussian random variables with zero-mean and unit variance $\mathcal{CN}(0,1)$. Therefore, the channel vectors can be described as $\mathbf{h}_{aw} \triangleq [h_{a_1w}, \cdots, h_{a_Mw}]^T \in \mathbb{C}^{M\times 1}$ between Alice and Willie, $\mathbf{h}_{ab} \triangleq [h_{a_1b}, \cdots, h_{a_Mb}]^T \in \mathbb{C}^{M\times 1}$ between Alice and Bob, and h_{bw} between Bob and Willie.

During each time slot, the channel coefficients are assumed to be constant, and vary independently from one slot to another. Assume that Alice has the channel state information (CSI) $\mathbf{h}_{ab}$[2]. Thus, she can optimize the precoding vector to maximize the received power at Bob as

$$\mathbf{v} = \frac{\mathbf{h}_{ab}^{\dagger}}{\|\mathbf{h}_{ab}\|}. \tag{1}$$

The signal symbols sent by Alice and the jamming symbols emitted by Bob can be denoted as $s[k]$ and $j[k]$, respectively, where $s[k]$, and $j[k]$ are i.i.d. complex Gaussian random variables with zero-mean and unit variance. $s[k]$ is precoded with $\mathbf{v}$ and then transmitted by Alice with the transmit power P_a, and $j[k]$ is emitted with the transmit power P_b by Bob. The received signals at Willie and Bob can be expressed as

$$y_w[k]=\sqrt{\frac{\rho_0 P_a}{r_{aw}^{\alpha}}}\mathbf{v}\mathbf{h}_{aw}s[k]+\sqrt{\frac{\rho_0 P_b}{r_{bw}^{\alpha}}}h_{bw}j[k]+n_w[k], \tag{2}$$

$$y_b[k] =\sqrt{\frac{\rho_0 P_a}{r_{ab}^{\alpha}}}\mathbf{v}\mathbf{h}_{ab}s[k]+\sqrt{\phi P_b}h_{bb}j[k]+n_b[k], \tag{3}$$

where $n_w[k]$ and $n_b[k]$ are the i.i.d. additive white Gaussian noise (AWGN) at Willie and Bob with variances of σ_w^2 and σ_b^2, respectively.

[2]The transmitter sends the training sequences to the receiver, and the estimated CSI at the receiver can be then fed back to the transmitter.

B. Connection Probability and Throughput

From Alice's point of view, she has to make sure that the transmission rate between her and Bob does not exceed the channel capacity to avoid errors, i.e., to avoid decoding errors at Bob. According to $y_b[k]$ given in (3), the received signal-to-interference-plus-noise-ratio (SINR) of Bob can be expressed as

$$\mathrm{SINR_b} = \frac{S_b}{J_b+\sigma_b^2}, \tag{4}$$

where $S_b = \rho_0 P_a |\mathbf{v}\mathbf{h}_{ab}|^2 r_{ab}^{-\alpha}$ is the received signal power from Alice, and $J_b = \phi P_b |h_{bb}|^2$ represents the self-interference power from himself. Thus, the maximum achievable transmission rate from Alice to Bob can be calculated as

$$R_{cap} = \ln\left(1+\mathrm{SINR_b}\right), \tag{5}$$

which is a random variable, due to $\|\mathbf{h}_{ab}\|^2$ and $|h_{bb}|^2$ in S_b and J_b, respectively.

When the transmission rate R is less than R_{cap}, the communication between Alice and Bob can perform reliably. Thus, we define the connection probability between Alice and Bob as [20]

$$P_c = \mathbb{P}\left\{R_{cap} \geq R\right\}. \tag{6}$$

To evaluate the connection of covert communication, the connection throughput can be defined as [20]

$$R_{cth} = P_c R. \tag{7}$$

III. Detection at Willie

Willie needs to decide whether Alice is talking to Bob or not by using the received signal $y_w[k]$. Specifically, Willie conducts a detection using hypothesis test to distinguish the null hypothesis $\mathcal{H}_0$ and its alternate hypothesis $\mathcal{H}_1$, where $\mathcal{H}_0$ indicates that Alice is silent, while $\mathcal{H}_1$ indicates transmission between Alice and Bob. The received signals at Willie in two hypotheses can be expressed as

$$y_w[k]=\begin{cases}\sqrt{\frac{\rho_0 P_b}{r_{bw}^{\alpha}}}h_{bw}j[k]+n_w[k], & \mathcal{H}_0,\\ \sqrt{\frac{\rho_0 P_a}{r_{aw}^{\alpha}}}\mathbf{v}\mathbf{h}_{aw}s[k]+\sqrt{\frac{\rho_0 P_b}{r_{bw}^{\alpha}}}h_{bw}j[k]+n_w[k], & \mathcal{H}_1.\end{cases} \tag{8}$$

False alarm (FA) indicates the acceptance of $\mathcal{H}_1$ when Alice is silent, while miss detection (MD) denotes the acceptance of $\mathcal{H}_0$ when there is a transmission between Alice and Bob. Willie uses an energy detector to test the average statistical power $\bar{P}_w$ of the received signals as

$$\bar{P}_w = \frac{1}{N}\sum_{k=1}^{N}|y_w[k]|^2. \tag{9}$$

Due to the averaging in (9), $\bar{P}_w$ tends to converge to a fixed value as the number of samples increases, i.e., $N\to\infty$. Thus, (9) becomes

$$\bar{P}_w \to \begin{cases} J_w+\sigma_w^2, & \mathcal{H}_0,\\ S_w+J_w+\sigma_w^2, & \mathcal{H}_1,\end{cases} \tag{10}$$

where $J_w = \rho_0 P_b |h_{bw}|^2 r_{bw}^{-\alpha}$ represents the received jamming power, and $S_w = \rho_0 P_a |\mathbf{h}_{aw}|^2 r_{aw}^{-\alpha}$ denotes the received power from Alice. We assume that J_w and S_w are unchanged during each time slot due to the quasi-static Rayleigh fading and fixed P_a and P_b.

Willie decides whether Alice is transmitting based on his observation [31]. The decision is made according to

$$\bar{P}_w \underset{\mathcal{D}_0}{\overset{\mathcal{D}_1}{\gtrless}} \xi, \tag{11}$$

where ξ is the predefined detection threshold of $\bar{P}_w$ at Willie, $\mathcal{D}_0$ denotes the decision of accepting $\mathcal{H}_0$, and $\mathcal{D}_1$ is in favor of $\mathcal{H}_1$. Willie decides $\mathcal{D}_0$ when $\bar{P}_w \leq \xi$, and $\mathcal{D}_1$ when $\bar{P}_w > \xi$. The probability of detection is calculated as [20]

$$p = p_{\mathcal{H}_0} \mathbb{P}\left\{\mathcal{D}_0 | \mathcal{H}_0\right\} + p_{\mathcal{H}_1} \mathbb{P}\left\{\mathcal{D}_1 | \mathcal{H}_1\right\}, \tag{12}$$

where $\mathbb{P}\{*\}$ means the probability of $*$ being true, $p_{\mathcal{H}_0} = \mathbb{P}\{\mathcal{H}_0\}$, and $p_{\mathcal{H}_1} = \mathbb{P}\{\mathcal{H}_1\}$. The classical literature [12] has proved that $p_{\mathcal{H}_0} = p_{\mathcal{H}_1} = 0.5$ can introduce more uncertainty to deceive Willie. Thus, we consider the equal priori probability of $p_{\mathcal{H}_0} = p_{\mathcal{H}_1} = 0.5$ in this paper, which indicates that Alice can transmit randomly in 50% of the time slots. Thus, (12) becomes

$$p = 0.5 \left(\mathbb{P}\left\{\mathcal{D}_0 | \mathcal{H}_0\right\} + \mathbb{P}\left\{\mathcal{D}_1 | \mathcal{H}_1\right\}\right). \tag{13}$$

The case when $p_{\mathcal{H}_0} \neq 0.5$ will be discussed in Appendix A.

Using $\bar{P}_w$ in (10) and the decision rule in (11), p can be calculated as

$$p = \begin{cases} 1, & J_w + \sigma_w^2 \leq \xi \leq S_w + J_w + \sigma_w^2, \\ 0.5, & \text{otherwise}, \end{cases} \tag{14}$$

where S_w and J_w are assumed to be unchanged for a specific time slot, and vary from slot to slot, due to the quasi-static Rayleigh fading and fixed P_a and P_b. Thus, p relies on the selection of ξ. As such, p becomes a standard Bernouli random variable with two possible outcomes $p = 1$ and $p = 0.5$ according to the given threshold ξ. This means either $\bar{P}_w = J_w + \sigma_w^2$ or $\bar{P}_w = S_w + J_w + \sigma_w^2$. When $J_w + \sigma_w^2 \leq \xi \leq S_w + J_w + \sigma_w^2$, we have $\mathbb{P}\{\mathcal{D}_0|\mathcal{H}_0\} = \mathbb{P}\{\mathcal{D}_1|\mathcal{H}_1\} = 1$, which leads to $p = 1$. When $\xi \leq J_w + \sigma_w^2$, we have $\mathbb{P}\{\mathcal{D}_0|\mathcal{H}_0\} = 0$ and $\mathbb{P}\{\mathcal{D}_1|\mathcal{H}_1\} = 1$, which leads to $p = 0.5$. Finally, when $\xi \geq S_w + J_w + \sigma_w^2$, we have $\mathbb{P}\{\mathcal{D}_0|\mathcal{H}_0\} = 1$ and $\mathbb{P}\{\mathcal{D}_1|\mathcal{H}_1\} = 0$, which also leads to $p = 0.5$.

If the transmission between Alice and Bob is discovered by Willie, the covert communication is not achievable. Therefore, we define the probability that the communication is found out by Willie as the covert outage probability p_o, which can be described as[3]

$$p_o = \mathbb{P}\{p = 1\}. \tag{15}$$

In an interference-limited network, we ignore σ_b^2 in (4) and σ_w^2 in (14).

IV. Optimal Threshold and Location for Willie

In this section, we analyze the metrics at Willie to find the optimal threshold and location for his detection.

[3] p_o can be calculated by taking the limit of infinite number of time slots.

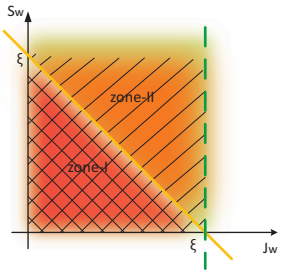

Fig. 2. Explanation of the CDF in (18).

A. Problem Formulation

Since Willie knows the location of Alice, his position will affect the correct detection probability. Thus, we optimize the position of Willie to achieve higher probability of detecting the transmission of Alice as

$$\begin{aligned} \textbf{P1:} \quad & \max_{\xi, \mathcal{W}} \; p_o && \text{(16a)} \\ & s.t. \;\; r_{aw} + r_{bw} \geq r_{ab}, && \text{(16b)} \\ & \quad\;\; r_{bw} \leq r_{aw} + r_{ab}, && \text{(16c)} \\ & \quad\;\; r \leq r_{aw} \leq r_0, && \text{(16d)} \\ & \quad\;\; r_{bw} > 0, && \text{(16e)} \end{aligned}$$

where r_{aw}, r_{bw}, and r_{ab} denote the distances from Alice to Willie, from Bob to Willie, and from Alice to Bob, respectively, with $r_{aw} = \|\mathcal{A} - \mathcal{W}\|$, $r_{bw} = \|\mathcal{B} - \mathcal{W}\|$, and $r_{ab} = \|\mathcal{A} - \mathcal{B}\|$. The constraints (16b) and (16c) result from the triangle inequality theorem, and the constraints (16d) and (16e) describe the possible locations of Willie. By solving (16), the optimal position for Willie can be found.

B. Optimal Detection Threshold

To solve the problem in (16), we need to derive the expression of p_o first, which can be derived by substituting (14) into (15) as

$$p_o = \mathbb{P}\left\{J_w \leq \xi \leq S_w + J_w\right\}. \tag{17}$$

As shown in Fig. 2, we first consider the case when $J_w \leq \xi$, which indicates the whole mesh zone-I and slash zone-II to the left of the green dotted line. In addition, $S_w + J_w$ has to be greater than ξ, which reduces the sum of zone-I and zone-II to the slash zone-II. Based on the basic knowledge of CDF, (17) can be calculated as

$$p_o = \mathcal{F}_{J_w}(\xi) - \mathcal{F}_{J_w + S_w}(\xi). \tag{18}$$

As $h_{bw} \sim \mathcal{CN}(0,1)$, we have $|h_{bw}|^2 \sim \exp(1)$ and

$$J_w \sim \exp(\lambda_b), \tag{19}$$

where $\lambda_b = \frac{r_{bw}^{\alpha}}{\rho_0 P_b}$. Thus, we have the CDF of J_w as

$$\mathcal{F}_{J_w}(\xi) = 1 - e^{-\lambda_b \xi}. \tag{20}$$

According to [32], with the i.i.d. distribution of $\mathbf{h}_{ab_i} \sim \mathcal{CN}(0,1)$ and $\mathbf{h}_{aw_i} \sim \mathcal{CN}(0,1)$, we have

$$\frac{|\mathbf{h}_{ab}^{\dagger} \mathbf{h}_{aw}|^2}{\|\mathbf{h}_{ab}\|^2} \sim \exp(1). \tag{21}$$

With the definition above, the distribution of S_w can be expressed as

$$S_w \sim \exp(\lambda_a), \tag{22}$$

where $\lambda_a = \frac{r_{aw}^{\alpha}}{\rho_0 P_a}$. Usually, $P_a \ll P_b$, and we have $\lambda_a \neq \lambda_b$. As S_w and J_w are i.i.d., p_o in (18) can be expressed as

$$\begin{aligned} p_o &= 1 - e^{-\lambda_b \xi} - \int_0^{\xi} \mathcal{F}_{J_w}(\xi - x) f_{S_w}(x)\, dx \\ &= \frac{\lambda_b}{\lambda_a - \lambda_b}\left(e^{-\lambda_b \xi} - e^{-\lambda_a \xi}\right), \qquad \lambda_a \neq \lambda_b. \end{aligned} \tag{23}$$

According to (23), we can conclude that p_o only depends on P_a, P_b, ξ and $\mathcal{W}$. To maximize p_o, the optimal detection threshold ξ^* is derived in Proposition 1.

Proposition 1: The optimal detection threshold ξ^* for Willie can be expressed as

$$\xi^* = \frac{\ln \lambda_a - \ln \lambda_b}{\lambda_a - \lambda_b}. \tag{24}$$

Proof: To derive the optimal detection threshold ξ^*, the monotonicity of p_o should be considered. Using p_o in (23), we have the first-order derivative of p_o with respect to ξ as

$$p_o'(\xi) = \frac{\lambda_b}{\lambda_a - \lambda_b}\left(\lambda_a e^{-\lambda_a \xi} - \lambda_b e^{-\lambda_b \xi}\right). \tag{25}$$

From the definitions of λ_a and λ_b, we know that $\lambda_a > 0$ and $\lambda_b > 0$.

First, if $\lambda_a > \lambda_b$, when $\xi < \xi^*$, we have $\lambda_a e^{-\lambda_a \xi} > \lambda_b e^{-\lambda_b \xi}$, and we further conclude that $p_o' > 0$. On the other hand, when $\xi > \xi^*$ we know that p_o' is negative.

If $\lambda_a < \lambda_b$, we derive $\lambda_a e^{-\lambda_a \xi} < \lambda_b e^{-\lambda_b \xi}$ from $\xi < \xi^*$, which leads to $p_o' > 0$. Then, $\xi > \xi^*$ can guarantee $p_o' < 0$.

Thus, p_o monotonically increases with ξ, when $\xi \leq \xi^*$, and monotonically decreases when $\xi > \xi^*$, based on which we can obtain the optimal detection threshold ξ^* to maximize p_o as (24). ∎

C. Optimal Detection Position

In practical systems, the jamming signal should be much stronger than the transmitted information, i.e., $P_a \ll P_b$, which leads to $\lambda_a \neq \lambda_b$. Thus, using the optimal ξ^* in (24), we can derive the optimal $p_o^{\triangle}$ as

$$p_o^{\triangle} = \left(\frac{\lambda_a}{\lambda_b}\right)^{-\frac{\lambda_a}{\lambda_a - \lambda_b}}, \qquad \lambda_a \neq \lambda_b. \tag{26}$$

Without loss of generality, assume that Bob is located at $\mathcal{B} = [x_a + r_{ab}, y_a]^T$. Then, we analyze the monotonicity of p_o against r_{aw} and r_{bw} in Proposition 2 to obtain the optimal detection location for Willie.

Proposition 2: The optimal detection location for Willie can be expressed as

$$\mathcal{W} = [x_a - r, y_a]^T. \tag{27}$$

Proof: From (26), we have the expression of $p_o^{\triangle}(\lambda_a)'$ and $p_o^{\triangle}(\lambda_b)'$ as

$$\frac{\partial p_o^{\triangle}}{\partial \lambda_a} = \frac{\lambda_b \left(\frac{\lambda_a}{\lambda_b}\right)^{-\frac{\lambda_a}{\lambda_a - \lambda_b}}}{(\lambda_a - \lambda_b)^2} t_{\lambda_a}, \tag{28a}$$

$$\frac{\partial p_o^{\triangle}}{\partial \lambda_b} = \frac{\lambda_a \left(\frac{\lambda_a}{\lambda_b}\right)^{-\frac{\lambda_a}{\lambda_a - \lambda_b}}}{(\lambda_a - \lambda_b)^2} t_{\lambda_b}, \tag{28b}$$

where we define

$$t_{\lambda_a} = \ln\left(\frac{\lambda_a}{\lambda_b}\right) - \frac{\lambda_a}{\lambda_b} + 1, \tag{29}$$

and

$$t_{\lambda_b} = -\ln\left(\frac{\lambda_a}{\lambda_b}\right) + \frac{\lambda_a}{\lambda_b} - 1. \tag{30}$$

With $\frac{\lambda_a}{\lambda_b} > 0$, we have $t_{\lambda_a}|_{\frac{\lambda_a}{\lambda_b} \to 0} < 0$, $t_{\lambda_a}|_{\frac{\lambda_a}{\lambda_b} = 1} = 0$, and $t_{\lambda_a}|_{\frac{\lambda_a}{\lambda_b} \to \infty} < 0$. Thus, it is obvious that $t_{\lambda_a} \leq 0$ and $t_{\lambda_b} \geq 0$, and we can further conclude that $p_o^{\triangle}$ monotonically decreases with λ_a while increasing with λ_b. Consequently, to obtain higher successful detection probability, Willie needs to make r_{aw} as small as possible while r_{bw} as large as possible.

With fixed r_{aw}, we can derive the optimal $r_{bw}^* = r_{aw} + r_{ab}$ from the coupling relationship of $r_{bw} \leq r_{aw} + r_{ab}$. Therefore, we have the first-order derivative of $p_o^{\triangle}(r_{aw})$ as

$$\begin{aligned} \frac{\partial p_o^{\triangle}}{\partial r_{aw}} &= \frac{\partial p_o^{\triangle}}{\partial \lambda_a}\frac{\partial \lambda_a}{\partial r_{aw}} + \frac{\partial p_o^{\triangle}}{\partial \lambda_b}\frac{\partial \lambda_b}{\partial r_{aw}} \\ &= \frac{p_o^{\triangle} \alpha (r_{aw} + r_{ab})^{\alpha - 1} (r_{aw})^{\alpha - 1} r_{ab} P_a P_b}{\left(P_b r_{aw}^{\alpha} - P_a (r_{aw} + r_{ab})^{\alpha}\right)^2} t_{\lambda_a}. \end{aligned} \tag{31}$$

As $t_{\lambda_a} \leq 0$, we can conclude from (31) that $\frac{\partial p_o^{\triangle}}{\partial r_{aw}} \leq 0$. Thus, the optimal position to maximize the successful detection probability p_o is $r_{aw}^* = r$. Then, we can further derive $r_{bw}^* = r + r_{ab}$, which leads to the optimal detection location for $\mathcal{W}$ expressed in (27). ∎

Thus, using the optimal detection threshold ξ^* in (24) and the optimal detection position in (27), the optimal detection probability p_o^* of Willie is

$$p_o^* = \left(\frac{r^{\alpha} P_b}{(r + r_{ab})^{\alpha} P_a}\right)^{-\frac{r^{\alpha}/P_a}{r^{\alpha}/P_a - (r + r_{ab})^{\alpha}/P_b}}. \tag{32}$$

Remark 1: Willie can obtain the optimal detection threshold as ξ^* based on Proposition 1, and perform the detection at the optimal location $\mathcal{W}^*$ demonstrated in Proposition 2. Accordingly, he can maximize his detection probability p_o based on these results in (24) and (27).

V. Covert Communication With Optimal Threshold and Position of Willie

In this section, we optimize the transmission rate, the transmit power and the jamming power to maximize the connectivity throughput with a fixed covert outage probability, in the worst situation when Willie operates with the optimal threshold and position[4].

[4]Although Willie can change his locations for detection, Alice tries to improve the covert performance assuming Willie at his optimal location.

A. Problem Formulation

The optimization problem can be formulated as

$$\mathbf{P2:}\ \max_{P_a,P_b,R}\ R_{cth} \tag{33a}$$
$$s.t.\quad P_a \le P_{a_{max}}, \tag{33b}$$
$$P_b \le P_{b_{max}}, \tag{33c}$$
$$R \ge R_{th}, \tag{33d}$$
$$p_o^* \le \varepsilon, \tag{33e}$$

where ε is the maximum allowed covert outage probability, R_{th} represents the rate threshold for Bob to correctly decode the message from Alice, and $P_{a_{max}}$ and $P_{b_{max}}$ are the maximum transmit power for Alice and Bob, respectively.

According to (6) and (7), R_{cth} is related to R and P_c, while P_c is also determined by R. Owing to the coupling between R and P_c, we first optimize P_a and P_b to obtain the maximum P_c^*. Then, R_{cth} is maximized by optimizing R. Consequently, the problem of (33) can be divided into two sub-problems as

$$\mathbf{P\ 2.1:}\ \max_{P_a,P_b}\ P_c \tag{34a}$$
$$s.t.\quad P_a \le P_{a_{max}}, \tag{34b}$$
$$P_b \le P_{b_{max}}, \tag{34c}$$
$$p_o^* \le \varepsilon, \tag{34d}$$

$$\mathbf{P\ 2.2:}\ \max_{R}\ R_{cth}, \tag{35a}$$
$$s.t.\quad P_c = P_c^*, \tag{35b}$$
$$R \ge R_{th}. \tag{35c}$$

The solution to P 2.1 is derived in Section V-B. With the optimal P_c^*, the connection throughput between Alice and Bob is maximized in Section V-C by solving P 2.2.

B. Connection Probability

According to (4) and (5), we can rewrite (6) as

$$P_c = \mathbb{P}\left\{\frac{S_b}{J_b+\sigma_b^2} \ge \beta\right\}, \tag{36}$$

where $\beta = e^R - 1 > 0$. Ignoring σ_b^2, (36) becomes

$$P_c = \mathbb{E}_{J_b}\left[\mathbb{P}\left\{\|\mathbf{h}_{ab}\|^2 \ge \gamma J_b\right\}\right], \tag{37}$$

where $\gamma = \frac{\beta r_{ab}^{\alpha}}{\rho_0 P_a}$. Since $h_{ab_i} \sim \mathcal{CN}(0,1)$ and $h_{bb} \sim \mathcal{CN}(0,1)$, we have $\|\mathbf{h}_{ab}\|^2 \sim \Gamma(M,1)$ and $|h_{bb}|^2 \sim \exp(1)$. Thus, we can obtain $J_b \sim \exp\left(\frac{1}{\phi P_b}\right)$. Then, (37) can be calculated as

$$\begin{aligned} P_c &= \mathbb{E}_{J_b}\left[e^{-\gamma J_b}\sum_{m=0}^{M-1}\frac{(\gamma J_b)^m}{m!}\right] \\ &= \sum_{m=0}^{M-1}\frac{\gamma^m}{m!}\frac{m!}{\left(\gamma+\frac{1}{\phi P_b}\right)^{m+1}P_b\phi} \\ &= 1-\left(1+\frac{\rho_0 P_a}{\phi P_b r_{ab}^{\alpha}(e^R-1)}\right)^{-M}. \end{aligned} \tag{38}$$

Then, we analyze the monotonicity of P_c with regard to P_a, P_b, R and M. From the expression of (38), we have the first-order derivative of P_c against P_a, P_b, M, and R as

$$\frac{\partial P_c}{\partial P_a} = \frac{M}{\phi P_b r_{ab}^{\alpha}\beta}\eta^{-M-1}, \tag{39a}$$
$$\frac{\partial P_c}{\partial P_b} = \frac{-M\rho_0 P_a}{\phi P_b^2 r_{ab}^{\alpha}\beta}\eta^{-M-1}, \tag{39b}$$
$$\frac{\partial P_c}{\partial M} = \eta^{-M}\ln\eta, \tag{39c}$$
$$\frac{\partial P_c}{\partial R} = \frac{-M\rho_0 P_a e^R}{\phi P_b r_{ab}^{\alpha}\beta^2}\eta^{-M-1}, \tag{39d}$$

where

$$\eta = 1+\frac{\rho_0 P_a}{\phi P_b r_{ab}^{\alpha}(e^R-1)}. \tag{40}$$

Thus, $\eta > 1$. We have $\frac{\partial P_c}{\partial P_a} > 0$, $\frac{\partial P_c}{\partial P_b} < 0$, $\frac{\partial P_c}{\partial M} > 0$, and $\frac{\partial P_c}{\partial R} < 0$. Thus, we can conclude that P_c monotonically increases with P_a and M, and decreases with P_b and R.

Accordingly, we can improve P_c by adjusting the transmit power and the number of antennas at Alice, the jamming power at Bob, and the transmission rate between them.

With $P_c'(M)$ given in (39c), we further discuss the influence of the number of antennas on the connection performance between Alice and Bob.

$P_c'(M)$ in (39c) suggests that P_c monotonically increases with M. The second-order derivative of $P_c(M)$ can be derived as

$$P_c''(M) = -(\ln\eta)^2\eta^{-M}. \tag{41}$$

Since $P_c''(M) < 0$, $P_c'(M)$ monotonically decreases with M. Based on $P_c'(M) > 0$ given in (39c), we know that with the increase of M, $P_c(M)$ becomes large but the increase tends to slow down. Therefore, we can conclude that P_c is concave with M. This suggests that more antennas equipped at Alice can improve P_c. However, the improvement becomes marginal as the number increases. Since the influence of the number of antennas on P_c decreases when M gets larger, M should be properly selected to achieve more effective communication. This will be further discussed in Section VI.

From p_o in (32), we can also see that it can be influenced by both P_a and P_b. To analyze the monotonicity of p_o^* against P_a and P_b, we derive its first-order derivatives with P_a and P_b as

$$\frac{\partial p_o^*}{\partial P_a} = \frac{\partial p_o^*}{\partial \lambda_a}\frac{\partial \lambda_a}{\partial P_a} = -p_o^{\triangle}(\lambda_a)'\frac{r^{\alpha}}{\rho_0 P_a^2}, \tag{42a}$$
$$\frac{\partial p_o^*}{\partial P_b} = \frac{\partial p_o^*}{\partial \lambda_b}\frac{\partial \lambda_b}{\partial P_b} = -p_o^{\triangle}(\lambda_b)'\frac{(r+r_{ab})^{\alpha}}{\rho_0 P_b^2}, \tag{42b}$$

where $\lambda_a = \frac{r^{\alpha}}{\rho_0 P_a}$ and $\lambda_b = \frac{(r+r_{ab})^{\alpha}}{\rho_0 P_b}$ according to Proposition 2. Since $p_o^{\triangle}(\lambda_a)' \le 0$ and $p_o^{\triangle}(\lambda_b)' \ge 0$, we have $p_o^*(P_a)' \ge 0$ and $p_o^*(P_b)' \le 0$. Thus, we can conclude that p_o^* monotonically increases with P_a, and decreases with P_b.

The influences of P_a and P_b on P_c are opposite to p_o^*. In order to bind the connection and derive the bounds of P_a and P_b from (34d), we first introduce an auxiliary variable as

$$t = \frac{\lambda_b}{\lambda_a} = \left(\frac{r+r_{ab}}{r}\right)^{\alpha}\frac{P_a}{P_b}. \tag{43}$$

It is obvious that $t > 0$. By deriving the upper bound of t, the maximum power ratio P_a/P_b can be obtained, which is presented in Proposition 3.

Proposition 3: The upper bound of the transmit-to-jamming power ratio P_a/P_b can be expressed as

$$\frac{P_a}{P_b} \leq \frac{r^\alpha}{(r+r_{ab})^\alpha} \frac{\mathscr{W}_0(\varepsilon \ln \varepsilon)}{\ln \varepsilon}, \tag{44}$$

where $\mathscr{W}_0(*)$ is the principal branch of Lambert W function [33].

Proof: Since $t = \frac{\lambda_b}{\lambda_a}$, p_o^* can be turned into

$$p_o^* = \left(\frac{1}{t}\right)^{-\frac{1}{1-t}}. \tag{45}$$

Substituting (45) into (34d), we have

$$\frac{1}{1-t} \ln t \leq \ln \varepsilon, \tag{46}$$

where $t \neq 1$. For simplicity, let $c = \ln \varepsilon$. Owing to $\varepsilon \in (0,1)$, we have $c \in (-\infty, 0)$. The upper bound of t is discussed in two situations of $t \in (0,1)$ and $t \in (1, +\infty)$.

First, when $t \in (1, +\infty)$, (46) can be changed to

$$\begin{aligned} \ln t &\geq (1-t)\, c, \\ cte^{ct} &\leq ce^c. \end{aligned} \tag{47}$$

Since $c < 0$, we have

$$-\frac{1}{e} \leq ce^c < 0. \tag{48}$$

Thus, the solution to (47) can be derived as

$$\frac{\mathscr{W}_{-1}(ce^c)}{c} \leq t \leq \frac{\mathscr{W}_0(ce^c)}{c}, \tag{49}$$

where $\mathscr{W}_{-1}(*)$ is the negative branch of Lambert W function. Based on the rule of Lambert W function, we have $\mathscr{W}_{-1}(ce^c) < -1 < \mathscr{W}_0(ce^c) < 0$, which leads to $\mathscr{W}_{-1}(ce^c) = c$. Therefore, we can conclude that

$$\frac{\mathscr{W}_{-1}(ce^c)}{c} \leq t \leq \frac{\mathscr{W}_0(ce^c)}{c} = 1, \tag{50}$$

which is against our original assumption of $t \in (1, +\infty)$.

Then, when $t \in (0,1)$, (46) can be turned to

$$\begin{aligned} \ln t &\leq (1-t)\, c, \\ cte^{ct} &\geq ce^c. \end{aligned} \tag{51}$$

The solution to (51) can be described as

$$t \in \left(0, \frac{\mathscr{W}_0(ce^c)}{c}\right) \bigcup \left(\frac{\mathscr{W}_{-1}(ce^c)}{c}, 1\right). \tag{52}$$

However, by realizing $\frac{\mathscr{W}_{-1}(ce^c)}{c} = 1$, the solution to (51) should be changed to $t \in \left(0, \frac{\mathscr{W}_0(ce^c)}{c}\right)$.

To sum up, the upper bound of t can be described as

$$0 < t \leq \frac{\mathscr{W}_0(\varepsilon \ln \varepsilon)}{\ln \varepsilon}. \tag{53}$$

Combining (43) and (53), the limit of the transmit-to-jamming power ratio can be derived as (44). ∎

Based on (43) and the optimal location of Willie in Proposition 2, P_c in (38) can be rewritten as

$$P_c = 1 - \left(1 + \frac{\rho_0 r^\alpha t}{\phi (r+r_{ab})^\alpha r_{ab}^\alpha \beta}\right)^{-M}. \tag{54}$$

Then, we have the first-order derivative of P_c against t as

$$\frac{\partial P_c}{\partial t} = \frac{\rho_0 r^\alpha M}{\phi (r+r_{ab})^\alpha r_{ab}^\alpha \beta} \eta^{-M-1}, \tag{55}$$

based on which, we have $\frac{\partial P_c}{\partial t} > 0$ according to the definition of η in (40). Therefore, the closed-form expression of P_c can be obtained for P 2.1 by applying $t = \frac{\mathscr{W}_0(\varepsilon \ln \varepsilon)}{\ln \varepsilon}$ as

$$P_c^* = 1 - \left(1 + \frac{\rho_0 r^\alpha \mathscr{W}_0(\varepsilon \ln \varepsilon)}{\phi (r+r_{ab})^\alpha r_{ab}^\alpha \beta \ln \varepsilon}\right)^{-M}. \tag{56}$$

Remark 2: With the power ratio of $\frac{P_a}{P_b}$ set as the upper bound in (44), the connection probability P_c can be maximized while guaranteeing the covertness requirement of p_o. Therefore, the legitimate users can achieve higher connection throughput by properly setting P_a, P_b and R.

C. Connection Throughput

In this subsection, to derive the solution to P 2.2, we calculate the connection throughput R_{cth} using the derived optimal P_c^* subject to a limit on the covert outage probability ε. Based on P_c^* in (56), the connection throughput is

$$\begin{aligned} R_{cth}(\beta) &= P_c^* R \\ &= \left[1 - \left(\frac{\mu\beta}{1+\mu\beta}\right)^M\right] \ln(1+\beta), \end{aligned} \tag{57}$$

where

$$\mu = \frac{\phi r_{ab}^\alpha}{\rho_0} \frac{(r+r_{ab})^\alpha}{r^\alpha} \frac{\ln \varepsilon}{\mathscr{W}_0(\varepsilon \ln \varepsilon)}. \tag{58}$$

To maximize the covert connection throughput, we analyze the monotonicity of $R_{cth}(\beta)$ against the transmission rate R. Before discussing the monotonicity of $R_{cth}(\beta)$, we first introduce Lemma 1.

Lemma 1: When $\mu \ll 1$, if a solution to $\frac{\partial R_{cth}(\beta)}{\partial \beta} = 0$ exists, it is unique.

Proof: In order to derive the tendency of $R_{cth}(\beta)$ with β, we first calculate its first-order derivative $R'_{cth}(\beta_0)$ as

$$\frac{\partial R_{cth}(\beta)}{\partial \beta} = \frac{1 - \left(\frac{\mu\beta}{1+\mu\beta}\right)^M}{1+\beta} - \frac{\mu M \ln(1+\beta)}{(1+\mu\beta)^2} \left(\frac{\mu\beta}{1+\mu\beta}\right)^{M-1}. \tag{59}$$

According to the principle of *l'Hôpital's* rule [34], we have

$$\lim_{\beta \to \infty} \left(\frac{\mu\beta}{1+\mu\beta}\right) = 1, \tag{60a}$$

$$\lim_{\beta \to 0} \left(\frac{\mu\beta}{1+\mu\beta}\right) = 0, \tag{60b}$$

$$\lim_{\beta \to \infty} \frac{\ln(1+\beta)}{(1+\mu\beta)^2} = 0, \tag{60c}$$

$$\lim_{\beta \to 0} \frac{\ln(1+\beta)}{(1+\mu\beta)^2} = 0. \tag{60d}$$

Thus, we conclude that

$$\lim_{\beta\to 0}\frac{\partial R_{cth}\left(\beta\right)}{\partial\beta}=1, \tag{61}$$

$$\lim_{\beta\to \infty}\frac{\partial R_{cth}\left(\beta\right)}{\partial\beta}=0. \tag{62}$$

If $\frac{\partial R_{cth}(\beta)}{\partial\beta}=0$ exists, assume that β_0 is one of the zero point roots. According to (59), we have

$$\frac{1-\left(1+\frac{1}{\mu\beta_0}\right)^{-M}}{1+\beta_0}=\frac{M\ln\left(1+\beta_0\right)\left(1+\frac{1}{\mu\beta_0}\right)^{-M-1}}{\mu\beta_0^2}. \tag{63}$$

The second-order derivative $R''_{cth}(\beta)$ is presented as (64) at the top of next page. Based on (63), $R''_{cth}(\beta)$ at β_0 can be derived as (65) at the top of next page, where

$$K(\beta_0)=\frac{M\ln(1+\beta_0)\left(1+\frac{1}{\mu\beta_0}\right)^{-M-1}}{\mu\beta_0^2}, \tag{66}$$

$$T(\beta_0)=\left(\frac{-(M+1)}{\beta_0(\mu\beta_0+1)}+\frac{2}{\beta_0}-\frac{2}{(\beta_0+1)\ln\left(1+\beta_0\right)}-\frac{1}{1+\beta_0}\right). \tag{67}$$

It is easy to see $K(\beta_0)>0$.

From the definition of μ in (58), we have $\mu\ll 1$ according to the related practical parameters. Based on $\ln(1+\beta_0)\le\beta_0$ and $\mu\ll 1$, we can conclude

$$T(\beta_0)<\frac{\beta_0-\frac{M-1}{\mu}-2}{\beta_0(\beta_0+\frac{1}{\mu})}. \tag{68}$$

As $\frac{M-1}{\mu}+2$ is very large, we have $\frac{\beta_0-\frac{M-1}{\mu}-2}{\beta_0(\beta_0+\frac{1}{\mu})}<0$, which indicates $T(\beta_0)<0$. Then, we conclude that $R''_{cth}(\beta_0)<0$, which indicates that $R'_{cth}(\beta)$ monotonically decreases around β_0. Thus, the zero point β_0 is unique. ■

With Lemma 1, the monotonicity of $R_{cth}\left(\beta\right)$ is proved in Proposition 4.

Proposition 4: $R_{cth}\left(\beta\right)$ first increases and then decreases with β.

Proof: With the limit in (60c), we have

$$\lim_{\beta\to 0}R_{cth}\left(\beta\right)=0, \tag{69}$$

When $\beta\to\infty$, the limit of $R_{cth}(\beta)$ can be expressed as

$$\begin{aligned}\lim_{\beta\to\infty}R_{cth}\left(\beta\right)&=\lim_{\beta\to\infty}\frac{1-\left(\frac{\mu\beta}{1+\mu\beta}\right)^{M}}{\frac{1}{\ln\left(1+\beta\right)}}\\&=\lim_{\beta\to\infty}\frac{-M\left(\frac{\mu\beta}{1+\mu\beta}\right)^{M-1}\frac{\mu}{(1+\mu\beta)^2}}{-\frac{1}{(1+\beta)(\ln(1+\beta))^2}}\\&=M\lim_{\beta\to\infty}\frac{\left(\ln\left(1+\beta\right)\right)^2}{1+\mu\beta}=0.\end{aligned} \tag{70}$$

In addition, as shown in (61) and (62), we can conclude that $\frac{\partial R_{cth}(\beta)}{\partial\beta}$ can be either positive when $\beta>0$ as shown in Fig. 3(a), or has a single zero point as shown in Fig. 3(b), according to Lemma 1.

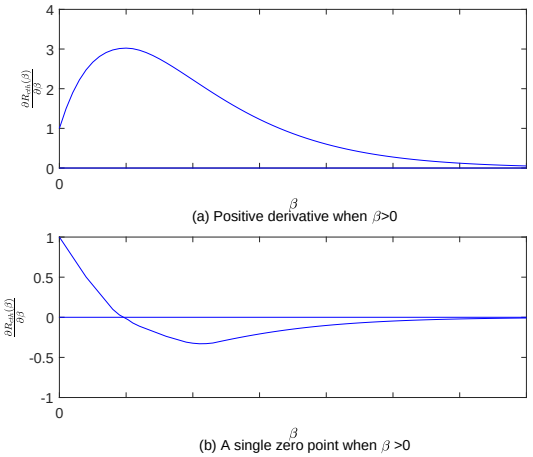

Fig. 3. The assumption of the tendency for $\frac{\partial R_{cth}(\beta)}{\partial\beta}$.

First, if the case in Fig. 3(a) is true, $R_{cth}\left(\beta\right)$ monotonically increases with β. According to (69), $R_{cth}\left(\beta\right)$ increases gradually from 0 as β gets larger. This contradicts with the fact in (70) that $R_{cth}\left(\beta\right)$ approaches to 0 when $\beta\to\infty$. Thus, this case is not true.

Consequently, Fig. 3(b) is true, and there exists a β_0 that leads to $\frac{\partial R_{cth}(\beta)}{\partial\beta}|_{\beta=\beta_0}=0$. Under this assumption, combining (69) and (70), we can conclude that $R_{cth}\left(\beta\right)$ first monotonically increases and then monotonically decreases. ■

Thus, we have the maximum covert connection throughput $R_{cth}\left(\beta_0\right)$, where β_0 is derived from $R'_{cth}(\beta_0)=0$. However, it is difficult to find the zero point β_0, owing to the complex expression of $R'_{cth}(\beta)$. Thus, we adopt the bisection method to find β_0. We can obtain the root of $R'_{cth}\left(\beta\right)=0$ through iteratively bisecting the interval $[\beta_a,\beta_b]$, and then selecting the subinterval, where $R'_{cth}\left(\beta\right)$ changes sign. The midpoint in the bisection method can be calculated as

$$\beta_c=\frac{\beta_a+\beta_b}{2}. \tag{71}$$

The approaching process starts with $\beta_a=e^{R_{th}}-1$ and a given initial $\beta_b=\beta_{ini}$, and ends until the difference Δ of β meets the minimum required precision δ, where Δ is defined as

$$\Delta=\beta_b-\beta_a. \tag{72}$$

With the given limit of covert outage probability ε, the optimal transmit-to-jamming power ratio $(\frac{P_a}{P_b})^*$ can be derived. Then, the calculation of the optimal transmission rate R^* between Alice and Bob can be summarized as Algorithm 1 based on the bisection method.

Thus, the achievable maximum connectivity throughput R^*_{cth} in P 2.2 can be calculated with optimized R^* derived from Algorithm 1 as

$$R^*_{cth}=\left[1-\left(\frac{\mu(e^R-1)}{1+\mu(e^R-1)}\right)^M\right]R^*. \tag{73}$$

VI. Simulation Results and Discussion

In this section, simulation results are presented to verify the effectiveness of the proposed scheme. Without loss of

$$R''_{cth}(\beta)=\frac{M\ln(1+\beta)\left(1+\frac{1}{\mu\beta}\right)^{-M-1}}{\mu\beta^2}\left(\frac{-(M+1)\left(1+\frac{1}{\mu\beta}\right)^{-1}}{\mu\beta^2}+\frac{2}{\beta}-\frac{2}{(\beta+1)\ln(1+\beta)}\right)-\frac{1-\left(1+\frac{1}{\mu\beta}\right)^{-M}}{(1+\beta)^2}. \quad (64)$$

$$\begin{aligned}R''_{cth}(\beta_0)&=\frac{M\ln(1+\beta_0)\left(1+\frac{1}{\mu\beta_0}\right)^{-M-1}}{\mu\beta_0^2}\left(\frac{-(M+1)}{\beta_0(\mu\beta_0+1)}+\frac{2}{\beta_0}-\frac{2}{(\beta_0+1)\ln(1+\beta_0)}\right)-\frac{M\ln(1+\beta_0)\left(1+\frac{1}{\mu\beta_0}\right)^{-M-1}}{\mu\beta_0^2}\frac{1}{(1+\beta_0)} \quad (65)\\&=K(\beta_0)T(\beta_0).\end{aligned}$$

Algorithm 1 The bisection method for P 2.2

Input: r, α, M, ϕ r_{ab}, ε, β_a, β_b, δ
Output: R^*

```
Get μ from (58)
Δ ← ∞
while Δ ≥ δ do
    Get β_c from (71)
    Get R'_cth(β_a), R'_cth(β_c), R'_cth(β_b) from (59)
    if R'_cth(β_c) == 0 then
        Break
    else if R'_cth(β_a) R'_cth(β_c) > 0 then
        β_a = β_c
    else
        β_b = β_c
    end if
    Δ ← β_b − β_a
end while
β_0 ← β_c
R* ← ln(β_0 + 1)
return R*
```

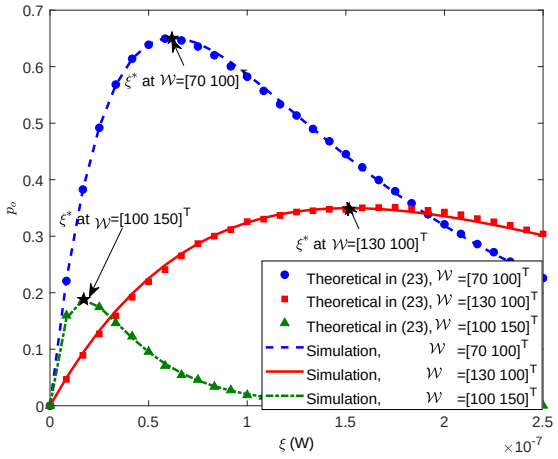

Fig. 4. Comparison of the covert outage probability p_o under different detection threshold ξ. Three cases of $\mathcal{W}=[70,100]^T$, $\mathcal{W}=[130,100]^T$ and $\mathcal{W}=[100,150]^T$ are considered.

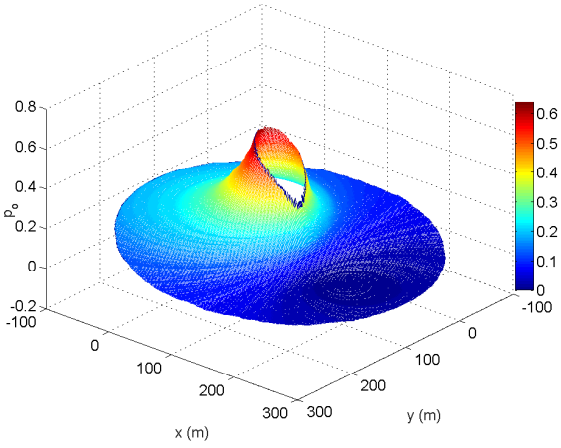

Fig. 5. Comparison of the covert outage probability p_o when Willie is located at different positions with the optimal ξ^*.

generality, assume that Alice and Bob are located at $\mathcal{A}=[100,100]^T$ and $\mathcal{B}=[200,100]^T$ in meters, respectively. The Willie wanders within the radius $r_0=200$ m around Alice, but stays outside of $r=30$ m. The channel coefficients follow Rayleigh fading with $\rho_0=-20$ dB and $\alpha=2.6$. The self-interference cancellation coefficient is $\phi=-90$ dB.

The covert outage probability is studied for different positions of Willie in Fig. 4, when $P_a=0.1$ W, $P_b=1$ W, and $M=8$. The results show that the theoretical values of p_o match with the simulation well. In addition, we can see that the covert outage probability first increases and then decreases with the detection threshold ξ. There exists an optimal detection threshold ξ^* to maximize p_o, which agrees with Proposition 1. Thus, we can conclude that different positions of Willie may lead to different p_o, which is further demonstrated in Fig. 5.

In Fig. 5, the covert outage probability p_o is studied when Willie is located at different positions using the optimal ξ^* set as (24), when $P_a=0.1$ W, $P_b=1$ W, and $M=8$. From the results, we can observe that the covert outage probability increases when Willie is closer to Alice and decreases when he gets closer to Bob. In addition, we can see that the covert outage probability reaches its maximum when Willie is at $[70,100]^T$ according to (27), which agrees with Proposition 2.

Then, the influence of P_a/P_b on the covert outage probability is investigated using the optimal ξ^* in (24) in Fig. 6, when $P_b=1$ W and $M=8$. From the results, we can observe that p_o monotonically increases with the power ratio P_a/P_b.

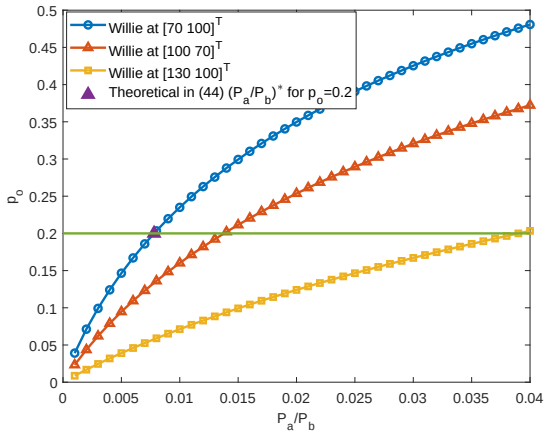

Fig. 6. Comparison of p_o with different P_a/P_b. $\mathcal{W} = [70, 100]^T$, $\mathcal{W} = [100, 70]^T$ and $\mathcal{W} = [130, 100]^T$ are considered. The theoretical maximum values of $(P_a/P_b)^*$ for $\varepsilon = 0.2$ are marked as well.

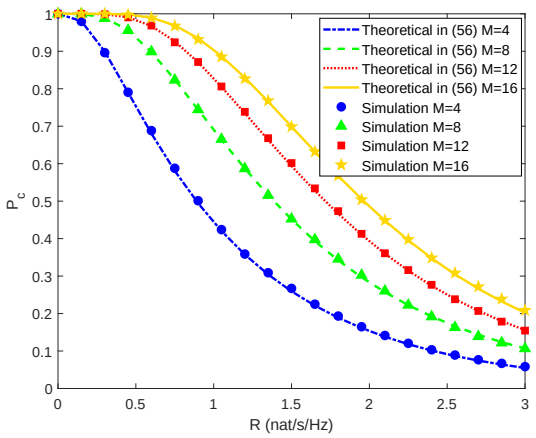

Fig. 7. Comparison of connection probability P_c with different transmission rate R. Four cases of $M = 4$, $M = 8$, $M = 12$ and $M = 16$ are considered.

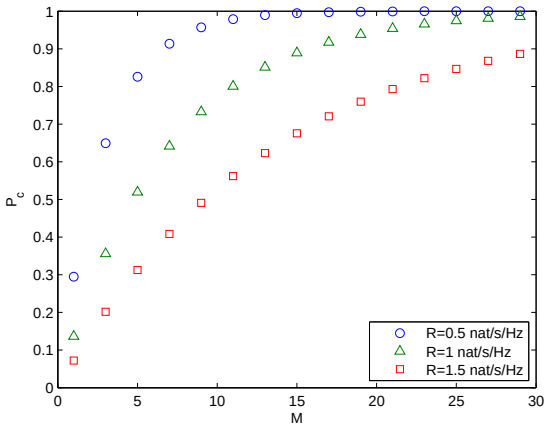

Fig. 8. Comparison of connection probability P_c for different M, with three cases $R = 0.5$ nat/s/Hz, $R = 1$ nat/s/Hz and $R = 1.5$ nat/s/Hz considered.

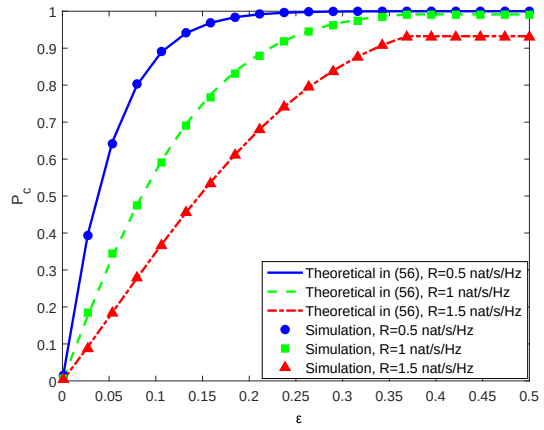

Fig. 9. Comparison of connection probability P_c for different covert outage limits, with three cases $R = 0.5$ nat/s/Hz, $R = 1$ nat/s/Hz and $R = 1.5$ nat/s/Hz considered.

In addition, we can also see that p_o is different when Willie is located at different positions. When $\mathcal{W} = [70, 100]^T$, p_o is the largest according to Proposition 2. With the upper bound of p_o set as $\varepsilon = 0.2$, the theoretical maximum value of P_a/P_b in (44) of Proposition 3 matches with the simulation result, where $\mathcal{W} = [70, 100]^T$.

In Fig. 7, the connection probability P_c is compared for different antenna numbers M at Alice, where $\varepsilon = 0.13$. Based on the upper bound of P_a/P_b in (44), we set $P_a = 0.0043$ W and $P_b = 1$ W. We can also see that P_c monotonically decreases with transmission rate R according to (39d). The results also indicate that the increase of number of antennas can lead to higher connection probability. Furthermore, we can see that the increasing of M will obviously affect the performance around $M = 16$ when $R > 1$ nat/s/Hz. However, when $M = 16$, the complexity of the transmitter is already very high, and we have no need to further improve the performance by increasing M. Based on this, the largest value of M is set to 16 for analysis, and we should make a balance between the complexity and the performance of covert communication when selecting M, which is further discussed in Fig. 8.

The impact of M on the connection probability P_c is investigated in Fig. 8 under different transmission rate R at Alice, when $P_a = 0.0043$ W and $P_b = 1$ W. We can see that P_c monotonically increases with M, and the increase tends to slow down as M becomes larger, which is consistent with the analysis in Section V-B. Thus, the performance improvement and the number of antennas should be carefully balanced.

The impact of covert outage upper bound ε on the connection probability P_c is investigated in Fig. 9, where $R = 0.5$ nat/s/Hz, $R = 1$ nat/s/Hz, and $R = 1.5$ nat/s/Hz are compared. We can see that P_c monotonically increases with ε, because larger ε will increase P_a/P_b. In addition, the results also indicate the better connection performance can be achieved with smaller transmission rate, which is consistent with that in Fig. 7.

Furthermore, the influence of the number of antennas and the upper bound of p_o on the connection throughput are investigated in Fig. 10 and Fig. 11, respectively, where $\mathcal{W} = [70, 100]^T$. In Fig. 10, we set $\varepsilon = 0.1$. From the results, we can see that the connection throughput first increases then

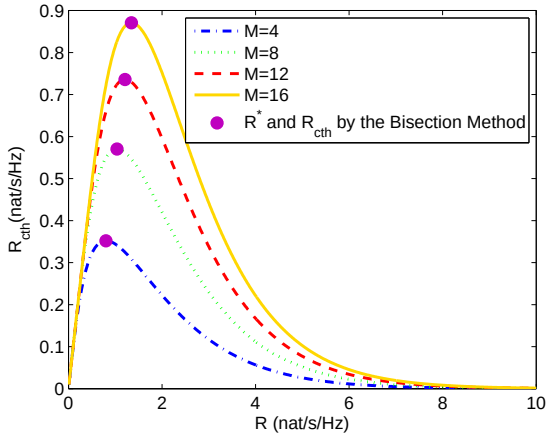

Fig. 10. Comparison of the connection throughput under different transmission rate R, with $M = 4$, $M = 8$, $M = 12$ and $M = 16$ considered. The optimal R^* and maximum R_{cth} derived by the bisection method are also presented.

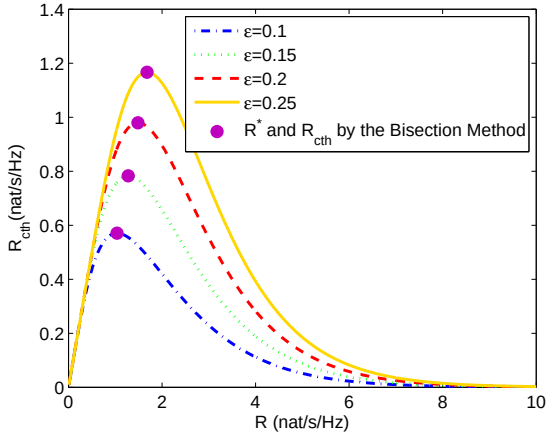

Fig. 11. Comparison of connection throughput under different transmission rate R, with $\varepsilon = 0.1$, $\varepsilon = 0.15$, $\varepsilon = 0.2$ and $\varepsilon = 0.25$ considered. The optimal R^* and the maximum R_{cth} derived by the bisection method are also presented.

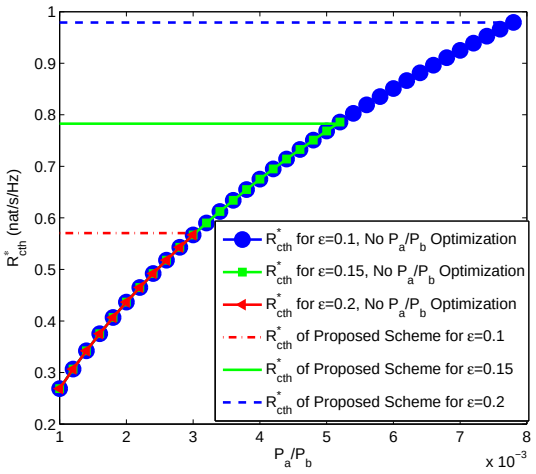

Fig. 12. Comparison of optimized connection throughput R^*_{cth} for the proposed scheme and the scheme without P_a/P_b optimization. Three cases of $\varepsilon = 0.1$, $\varepsilon = 0.15$ and $\varepsilon = 0.2$ are considered.

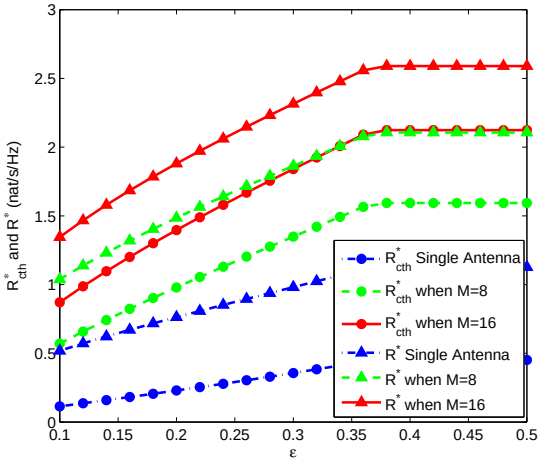

Fig. 13. Comparison of maximized connection throughput R^*_{cth} and optimized transmission rate R^* under different ε. Three cases of $M = 8$, $M = 16$ and single antenna are considered.

decreases with the transmission rate R. We can also find that the optimal values of R^* derived by the bisection method are consistent with the simulation ones. In addition, the results also show that the increase of M can achieve higher connection throughput. On the other hand, the connection throughput is compared with different covert outage limits in Fig. 11, with $\varepsilon = 0.1$, $\varepsilon = 0.15$, $\varepsilon = 0.2$ and $\varepsilon = 0.25$, respectively. We set $M = 8$. From the results, we can see that the increase of ε leads to higher connection throughput.

The connection throughput is compared for the proposed scheme and the scheme without P_a/P_b optimization in Fig. 12, with $M = 8$. From the results, we can see that the connection throughput increases with P_a/P_b until $p_o = \varepsilon$ in the scheme when the power ratio is not optimized, which can reach its maximum value as $p_o = \varepsilon$ in the proposed scheme. In addition, R^*_{cth} becomes higher with larger ε in the proposed scheme, due to the fact that the restriction on ε is relaxed to allow higher transmit power at Alice.

The maximum connection throughput R^*_{cth} and the optimal transmission rate R^* are compared for different number of antennas in Fig. 13 with varying ε. From the results, we can see that both R^*_{cth} and R^* increase with ε when it is small, but tend to be unchanged when ε becomes larger. This is because, P_c approaches 1 as ε keeps increasing, which leads to the stability of R^*_{cth} and R^*. In addition, we can also conclude that the proposed scheme with multiple antennas can achieve better performance than that when only a single antenna is equipped at Alice.

Finally, the effectiveness of the proposed scheme is verified towards location uncertainty in Fig. 14, when $M = 8$ and Willie is located at different positions adopting the optimal ξ^* set as (24). We set $P_a = 0.0043$ W and $P_b = 1$ W according to the upper bound of P_a/P_b in (44) when $\varepsilon = 0.13$. From the results, we can see that the maximum covert outage probability is achieved at Willie's optimal detection location

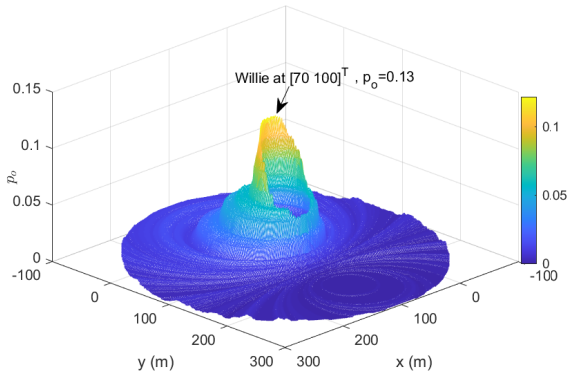

Fig. 14. Comparison of the covert outage probability p_o when Alice and Bob set their transmit power to their optimal as (44) and Willie is located at different positions with the optimal ξ^*.

$\mathcal{W} = [70, 100]^T$, which is consist with Proposition 2. In addition, although the location of Willie is uncertain, the covertness requirement $p_o \leq \varepsilon$ can be guaranteed wherever Willie locates, when Alice and Bob set their power ratio to the upper bound in (44). For the connection throughput, it will not affected by the location of Willie. Thus, we can conclude that the proposed scheme of covert communication is effective towards the location uncertainty of Willie.

VII. Conclusions

In this paper, we have considered the covert communication of a multi-antenna transmitter aided by a full-duplex jamming receiver against a warden with uncertain locations. To guarantee the covert outage probability lower than its limit while maximizing the connection throughput, a covert communication scheme is proposed. The optimal detection location and power threshold are presented for the warden to demonstrate the worst situation for the covert communication. Then, the transmit-to-jamming power ratio and the transmission rate are optimized sequentially to maximize the connection throughput under the given covert outage limit for this worst situation. Specifically, to calculate the optimal transmission rate, the bisection method is utilized. Simulation results are presented to prove that the theoretical results are perfectly consistent with the simulation ones, and the proposed scheme can maximize the connection throughput while guaranteeing the covertness effectively.

Appendix A
Applicability of p when $p_{\mathcal{H}_0} \neq p_{\mathcal{H}_1}$

Based on [35], when $p_{\mathcal{H}_0} = p_{\mathcal{H}_1} = 0.5$, we have the upper limit of Willie's correct detection probability as

$$p = \frac{1}{2}(\mathbb{P}_{FA} + \mathbb{P}_{MD}) \leq 0.5 + \varepsilon. \tag{74}$$

where $\mathbb{P}_{FA}$ is the probability of FA, and $\mathbb{P}_{MD}$ is the probability of MD.

On the other hand, when $p_{\mathcal{H}_0} \neq p_{\mathcal{H}_1}$, Alice can still carry covert communication with Bob. In this case, the detection probability of Willie can be calculated as

$$\begin{aligned} p^* &= p_{\mathcal{H}_0}\mathbb{P}\left\{J_w + \sigma_w^2 \leq \xi\right\} + p_{\mathcal{H}_1}\mathbb{P}\left\{S_w + J_w + \sigma_w^2 \geq \xi\right\} \\ &= (1 - p_{\mathcal{H}_1})(1 - \mathbb{P}_{FA}) + p_{\mathcal{H}_1}(1 - \mathbb{P}_{MD}) \\ &\leq 1 - \min\{1 - p_{\mathcal{H}_1}, p_{\mathcal{H}_1}\}(\mathbb{P}_{FA} + \mathbb{P}_{MD}) \\ &\leq 1 - \min\{1 - p_{\mathcal{H}_1}, p_{\mathcal{H}_1}\} + \varepsilon', \end{aligned} \tag{75}$$

where $\varepsilon' = 2\varepsilon \min\{1 - p_{\mathcal{H}_1}, p_{\mathcal{H}_1}\}$. We can see that the maximum p when $p_{\mathcal{H}_0} = p_{\mathcal{H}_1} = 0.5$ is smaller than p^* when $p_{\mathcal{H}_0} \neq p_{\mathcal{H}_1}$. Thus, we set $p_{\mathcal{H}_0} = p_{\mathcal{H}_1} = 0.5$ to improve the covert performance for Alice in the paper.

References

[1] D. Wang, D. Chen, B. Song, N. Guizani, X. Yu, and X. Du, "From IoT to 5G I-IoT: The next generation IoT-Based intelligent algorithms and 5G technologies," *IEEE Commun. Mag.*, vol. 56, no. 10, pp. 114–120, Oct. 2018.

[2] Y. Zhang, R. Woods, Y. Ko, A. Marshall, and J. Zhang, "Security optimization of exposure region-based beamforming with a uniform circular array," *IEEE Trans. Commun.*, vol. 66, no. 6, pp. 2630–2641, Jun. 2018.

[3] Y. Cao, N. Zhao, Y. Chen, M. Jin, Z. Ding, Y. Li, and F. R. Yu, "Secure transmission via beamforming optimization for NOMA networks," *IEEE Wireless Commun.*, vol. 27, no. 1, pp. 193–199, Feb. 2020.

[4] X. Yu, D. Xu, Y. Sun, D. W. K. Ng, and R. Schober, "Robust and secure wireless communications via intelligent reflecting surfaces," *IEEE J. Sel. Areas Commun.*, vol. 38, no. 11, pp. 2637–2652, Nov. 2020.

[5] T. Zheng, H. Wang, Q. Yang, and M. H. Lee, "Safeguarding decentralized wireless networks using full-duplex jamming receivers," *IEEE Trans. Wireless Commun.*, vol. 16, no. 1, pp. 278–292, Jan. 2017.

[6] A. Sheikholeslami, M. Ghaderi, H. Pishro-Nik, and D. Goeckel, "Energy-efficient secrecy in wireless networks based on random jamming," *IEEE Trans. Commun.*, vol. 65, no. 6, pp. 2522–2533, Jun. 2017.

[7] X. Zhou and Q. Wu and S. Yan and F. Shu and J. Li, "UAV-Enabled Secure Communications: Joint Trajectory and Transmit Power Optimization," *IEEE Trans. Veh. Tech.*, vol. 68, no. 4, pp. 4069–4073, Apr. 2019.

[8] X. Chen, D. Li, Z. Yang, Y. Chen, N. Zhao, Z. Ding, and F. R. Yu, "Securing aerial-ground transmission for NOMA-UAV networks," *IEEE Network*, vol. 34, no. 6, pp. 171–177, Nov.-Dec. 2020.

[9] S. Gong, C. Xing, S. Chen, and Z. Fei, "Polarization sensitive array based physical-layer security," *IEEE Trans. Veh. Tech.*, vol. 67, no. 5, pp. 3964–3981, May 2018.

[10] S. Gong, C. Xing, S. Chen, and Z. Fei, "Secure communications for dual-polarized MIMO systems," *IEEE Trans. Signal Process.*, vol. 65, no. 16, pp. 4177–4192, Aug. 2017.

[11] R. Anderson, *Information Hiding, First International Workshop, Cambridge, U.K., May 30 - June 1, 1996, Proceedings*. Springer-Verlag, 1996.

[12] B. A. Bash, D. Goeckel, and D. Towsley, "Limits of reliable communication with low probability of detection on AWGN channels," *IEEE J. Sel. Areas Commun.*, vol. 31, no. 9, pp. 1921–1930, Sept. 2013.

[13] D. Goeckel, B. Bash, S. Guha, and D. Towsley, "Covert communications when the warden does not know the background noise power," *IEEE Commun. Lett.*, vol. 20, no. 2, pp. 236–239, Feb. 2016.

[14] B. A. Bash, D. Goeckel, and D. Towsley, "Covert communication gains from adversarys ignorance of transmission time," *IEEE Trans. Wireless Commun.*, vol. 15, no. 12, pp. 8394–8405, Dec. 2016.

[15] B. He, S. Yan, X. Zhou, and V. K. N. Lau, "On covert communication with noise uncertainty," *IEEE Commun. Lett.*, vol. 21, no. 4, pp. 941–944, Apr. 2017.

[16] J. Hu, S. Yan, X. Zhou, F. Shu, J. Li, and J. Wang, "Covert communication achieved by a greedy relay in wireless networks," *IEEE Trans. Wireless Commun.*, vol. 17, no. 7, pp. 4766–4779, Jul. 2018.

[17] X. Zhou, S. Yan, J. Hu, J. Sun, J. Li, and F. Shu, "Joint optimization of a UAV's trajectory and transmit power for covert communications," *IEEE Trans. Signal Process.*, vol. 67, no. 16, pp. 4276–4290, Aug. 2019.

[18] S. Yan, X. Zhou, J. Hu, and S. V. Hanly, "Low probability of detection communication: opportunities and challenges," *IEEE Wireless Commun.*, vol. 26, no. 5, pp. 19–25, Oct. 2019.

[19] K. Shahzad, X. Zhou, and S. Yan, "Covert wireless communication in presence of a multi-antenna adversary and delay constraints," *IEEE Trans. Veh. Technol.*, vol. 68, no. 12, pp. 12432–12436, Dec. 2019.

[20] T. Zheng, H. Wang, D. W. K. Ng, and J. Yuan, "Multi-antenna covert communications in random wireless networks," *IEEE Trans. Wireless Commun.*, vol. 18, no. 3, pp. 1974–1987, Mar. 2019.

[21] J. Hu, Y. Wu, R. Chen, F. Shu, and J. Wang, "Optimal detection of UAV's transmission with beam sweeping in covert wireless networks," *IEEE Trans. Veh. Technol.*, vol. 69, no. 1, pp. 1080–1085, Jan. 2020.

[22] O. Shmuel and A. Cohen and O. Gurewitz and A. Cohen, "Multi-Antenna Jamming in Covert Communication," in *Proc. IEEE ISIT'19*, pp. 987–991, Paris, France, Jul. 2019.

[23] O. Shmuel, A. Cohen, O. Gurewitz, and A. Cohen, "Multi-antenna jamming in covert communication," in *Proc. IEEE ISIT'19*, pp. 987–991, Paris, France, Jul. 2019.

[24] R. Soltani, D. Goeckel, D. Towsley, B. A. Bash, and S. Guha, "Covert wireless communication with artificial noise generation," *IEEE Trans. Wireless Commun.*, vol. 17, no. 11, pp. 7252–7267, Nov. 2018.

[25] Z. Liu, J. Liu, Y. Zeng, and J. Ma, "Covert wireless communications in IoT systems: Hiding information in interference," *IEEE Wireless Commun.*, vol. 25, no. 6, pp. 46–52, Dec. 2018.

[26] R. Soltani, B. Bash, D. Goeckel, S. Guha, and D. Towsley, "Covert single-hop communication in a wireless network with distributed artificial noise generation," in *Proc. Allerton'14*, pp. 1078–1085, Monticello, IL, Sept. 2014.

[27] K. Shahzad, X. Zhou, S. Yan, J. Hu, F. Shu, and J. Li, "Achieving covert wireless communications using a full-duplex receiver," *IEEE Trans. Wireless Commun.*, vol. 17, no. 12, pp. 8517–8530, Dec. 2018.

[28] J. Hu, S. Yan, X. Zhou, F. Shu, and J. Li, "Covert wireless communications with channel inversion power control in Rayleigh fading," *IEEE Trans. Veh. Technol.*, vol. 68, no. 12, pp. 12135–12149, Dec. 2019.

[29] D. S. Karas, A. A. Boulogeorgos, and G. K. Karagiannidis, "Physical layer security with uncertainty on the location of the eavesdropper," *IEEE Wireless Commun. Lett.*, vol. 5, no. 5, pp. 540–543, Oct. 2016.

[30] M. Forouzesh, P. Azmi, N. Mokari, and D. Goeckel, "Covert communication using null space and 3D beamforming: Uncertainty of willie's location information," *IEEE Trans. Veh. Tech.*, vol. 69, no. 8, pp. 8568–8576, Aug. 2020.

[31] T. V. Sobers, B. A. Bash, S. Guha, D. Towsley, and D. Goeckel, "Covert communication in the presence of an uninformed jammer," *IEEE Trans. Wireless Commun.*, vol. 16, no. 9, pp. 6193–6206, Sept. 2017.

[32] T. Zheng, H. Wang, J. Yuan, D. Towsley, and M. H. Lee, "Multi-antenna transmission with artificial noise against randomly distributed eavesdroppers," *IEEE Trans. Commun.*, vol. 63, no. 11, pp. 4347–4362, Nov. 2015.

[33] R. M. Corless, G. H. Gonnet, D. Hare, D. J. Jeffrey, and D. E. Knuth, "On the lambertw function," *Advances in Computational Mathematics*, vol. 5, no. 1, pp. 329–359, 1996.

[34] G. de l'Hôpital, *Analyse Des Infiniment Petits Pour L'intelligence Des Lignes Courbes*. 1692.

[35] R. Soltani and D. Goeckel and D. Towsley and A. Houmansadr, "Fundamental Limits of Invisible Flow Fingerprinting," *IEEE Trans. Inf. Forens. Security*, vol. 15, pp. 345–360, May 2020.